Desalination and Water Treatment
www.deswater.com

doi: 10.5004/dwt.2017.20584

74 (2017) 216–223
May

Humic acid-carbon hybrid material as lead(II) ions adsorbent

Shaimaa T. El-Wakeel[a,*], Emad K. Radwan[a], Hany H. Abdel Ghafar[a,b], Ahmed S. Moursy[a]

[a]*Water Pollution Research Department, National Research Centre, 33 El Bohouth St, Dokki, Giza, Egypt 12622, Tel. +202 33370931; Fax: +202 33371211; emails: shaimaa_tw@yahoo.com (S.T. El-Wakeel), emadk80@gmail.com (E.K. Radwan), hany_ghafar@hotmail.com (H.H. Abdel Ghafar), ahmedsmoursy@yahoo.com (A.S Moursy)*
[b]*Department of Chemistry, Faculty of Sciences and Arts, Khulais, University of Jeddah, Saudi Arabia*

Received 8 September 2016; Accepted 6 February 2017

ABSTRACT

The current work represents the removal of lead from aqueous solution onto three adsorbents namely insolubilized humic acid (IHA), porous carbon (PC) and insolubilized humic acid mounted on porous carbon (IHPC). The effect of contact time, pH, adsorbent dose and the initial concentration of lead ions on the adsorption process were investigated. Freundlich, Langmuir and Dubinin–Radushkevich (D–R) isotherm models were implemented to describe the lead adsorption by the three adsorbents. The results showed that the Langmuir model was the best model to describe the adsorption of lead onto the adsorbents in current study. The Langmuir maximum adsorption capacities were 714.3, 454.5 and 333.3 mg/g for IHPC, IHA and PC, respectively. The obtained data followed the pseudo-second-order kinetic model. Adsorption energy values indicated that a chemisorption process takes place as supported by Fourier transform infrared analysis. The humic acid-carbon hybrid material (IHPC) exhibited much higher affinity and adsorption capacity for lead ions than the pure materials (IHA and PC) indicating that IHPC can be used as potential adsorbent for water treatment.

Keywords: Insolubilized humic acid; Porous carbon; Insolubilized humic acid mounted porous carbon; Adsorption; Lead ions

1. Introduction

Water contamination by heavy metals has gained more attention in the last decades due to the increased demand of heavy metals in many industries [1]. Lead is non-biodegradable and toxic, and causes nervous disorders, kidney diseases, anemia and death.

It exists in surface water due to its implementation in different types of industries such as mining, painting, pigments, plastic industries, industrial and domestic workflow, batteries, glass and steel, and alloy industries [1–3]. The widespread presence of lead and its adverse effects on human being and living organisms make it a serious environmental problem. The WHO guidelines indicated 0.01 mg/L as the permissible limit for Pb ions in drinking water [4,5]. Therefore, the research on the removal of Pb from aqueous solution is urgently needed to be kept within the permissible limits.

Lead can be removed from aqueous solutions by several methods such as adsorption, biosorption, chemical precipitation, ion exchange and membrane separation techniques [6,7]. However, the technical issues and economic feasibility retard the use of most of these methods [8]. Among these methods, adsorption is widely implemented due to the convenient design and operation conditions [6,8,9].

Adsorption of heavy metals on activated carbons gained much attention in the last decade due to its high surface area, large pore volume, high surface activity and existence of different types of active function groups, especially oxygen-containing groups, which are appropriate for the adsorption of metals such as Pb ions [8,10,11]. Moreover, activated carbon is thermally stable and inert, and can be used at different ranges of pH [12]. However, the cost of preparation and regeneration of activated carbon is considered high; therefore, it is considered as less economic adsorbent. Consequently, there is a continuous research for economical adsorbents for the removal of Pb ions and heavy metals from aqueous media.

---

* Corresponding author.

1944-3994/1944-3986

Currently, many researchers have been focused on humic acid as low-cost adsorbent. It can be extracted from peat, from soil and also on large scale from lignite. Humic acid has many advantages as adsorbent such as a large number of surface-active functional groups that make it a promising adsorbent for water and wastewater treatment. However, its solubility in water renders the application in water treatment [13]. To overcome the solubility of humic acid and high cost of activated carbons, we reported in our previous work a new hybrid materials gathering both humic acid and activated carbons [14]. These materials are insolubilized humic acid mounted porous carbon (IHPC) and carbon-coated humic acid. These hybrids have high affinity for adsorption of organic pollutants much higher than activated carbon and humic acid.

In the current work, porous carbon (PC), insolubilized humic acid (IHA) and IHPC were implemented for the adsorption of Pb ions from water. To check the capability of the new material (IHPC), the effect of pH, concentration of lead ions, contact time and dose of adsorbent have been investigated. A full comparison between IHPC, IHA and PC in adsorption of lead was conducted to prove the merit of the new material (IHPC).

2. Materials and methods

2.1. Chemicals

The chemicals used in the current study were of analytical grade and provided by Merck (Darmstadt, Germany). Stock Pb^{2+} solution of concentration 1,000 mg/L was prepared by dissolving an appropriate amount of $Pb(NO_3)_2$ in deionized water, and the volume was completed to 1 L. The working solutions were then prepared from the stock solution by dilution.

2.2. Preparation of adsorbents

The preparation procedures and characterization of the studied adsorbents (PC, IHA and IHPC) are described in other work [14].

2.3. Adsorption experiments

The batch adsorption studies were carried out by contacting the adsorbent with the synthetic Pb^{2+} solution in 100 glass reagent bottles. The experiments was conducted at room temperature (25°C ± 1.0°C) using a mechanical shaker at 200 rpm. All samples were filtered, and the Pb^{2+} concentration was measured in the filtrate. To distinguish between possible lead ions precipitation and actual lead adsorption, controls were used without adsorbent materials.

2.3.1. Effect of contact time

The effect of contact time was conducted by performing the batch adsorption experiments with an initial Pb^{2+} ions concentration of 20 mg/L and 0.5 g/L of adsorbent at different time intervals (5, 10, 30, 45,60, 90 and 120 min).

2.3.2. Effect of pH

The batch experiment was carried out at different pH value (from 2.3 to 6.2): below pH 2 the high proton concentration minimizes the metal adsorption, and above pH 6.5 Pb^{2+} precipitation is favored [15]. The pH of the solutions was adjusted either by 0.1 N hydrochloric acid or sodium hydroxide. The mixture was shaken for the optimum contact time and filtered, and the final pH of each sample was determined.

2.3.3. Effect of adsorbent dosage

The adsorbent dosages were varied from 0.05 to 1 g/L using a fixed volume of 100 mL of 20 mg/L of Pb^{2+} at the optimum pH and contact time.

2.4. Adsorption isotherms

Adsorption isotherm experiments were performed by shaking Pb^{2+} solutions of different concentrations (45–350 mg/L) using the optimum dose of each adsorbent for 25 min for PC and 30 min for IHA and IHPC at pH of 6.2.

The adsorption isotherm models are important in studying the interaction between adsorbent and adsorbate and to optimize the implementation of adsorbents. Freundlich, Langmuir and Dubinin–Radushkevich (D–R) isotherm are three different adsorption isotherms that were used to describe the data of lead adsorption onto PC, IHA and IHPC [16].

2.4.1. Langmuir and Freundlich isotherms

Langmuir and Freundlich equations are the most widely implemented models to describe the relationship between equilibrium metal uptake (q_e) and final concentrations (C_e) at equilibrium.

The linear form of Langmuir isotherm model is given by the relationship:

$$\frac{C_e}{q_e} = \frac{1}{q_{\max}K} + \frac{1}{q_{\max}}C_e \tag{1}$$

where K (L/g) is the equilibrium adsorption constant, which is related to the affinity of the binding sites, and $q_{\max}$ (mg/g) is the maximum amount of metal ion adsorbed per unit mass of adsorbent in case of occupation of all binding sites. The Langmuir parameters (K and $q_{\max}$) can be calculated by plotting C_e/q_e vs. C_e.

The logarithmic form of Freundlich equation is given by:

$$\log q_e = \log K_f + \frac{1}{n}\log C_e \tag{2}$$

where n and K_f are the Freundlich constants, which are related to the adsorption capacity of the adsorbent and the adsorption intensity.

2.4.2. Dubinin-Radushkevich (D–R) isotherm

The D–R isotherm is more general than Langmuir isotherm because it does not assume a homogeneous surface or constant potential of adsorption. The nature of adsorption process chemical or physical can be predicted from the D–R model. The linear form of the D–R isotherm equation can be expressed as follows:

$$\ln q_e = \ln X_m - \beta\varepsilon^2 \tag{3}$$

where q_e is the amount of lead ions adsorbed per unit mass of adsorbent (mol/g); X_m is the maximum adsorption capacity; β is the activity coefficient related to mean sorption energy (mol^2/kJ^2); and ε is the Polanyi potential that equal to:

$$\varepsilon = RT\ln\left(1+\frac{1}{C_e}\right) \tag{4}$$

where R is the general gas constant (J/mol K), and T is the absolute temperature (K). The adsorption energy can also be calculated by using the following equation:

$$E = \frac{1}{\sqrt{-2\beta}} \tag{5}$$

2.5. Adsorption kinetics

For adsorption kinetic tests, optimum dose of the tested adsorbents was added to Pb^{2+} solutions (20 mg/L) at pH of 6.2 for different time intervals. The kinetic data were fitted to pseudo-first-order, pseudo-first-order and Elovich models.

2.5.1. Pseudo-first-order model

The integrated form of the pseudo-first-order kinetic model can be expressed as follows [17]:

$$\log(q_e - q_t) = \log q_e - \frac{k_1 t}{2.303} \tag{6}$$

where q_e (mg/g) and q_t are the amounts of metal ions adsorbed on the adsorbent at equilibrium and at a time t, respectively, while k_1 is the rate constant of the first-order adsorption model (min^{-1}).

If the pseudo-first-order kinetics can be applied, the plot of log ($q_e - q_t$) vs. t shall provide a linear relationship from which k_1 and predicted q_e can be calculated from the intercept and slope of the plot.

2.5.2. Pseudo-second-order model

The linear form of the pseudo-second-order model equation is expressed as follows [18]:

$$\frac{t}{q_t} = \frac{1}{k_2} + \frac{1}{q_e}t \tag{7}$$

where k_2 is the rate constant (g/mg min).

2.5.3. Elovich model

The Elovich kinetic model can be expressed by the following equation [19]:

$$q_e = \frac{1}{\beta}\ln(\alpha\beta) + \frac{1}{\beta}\ln(t) \tag{8}$$

where α (mg/g min) is the initial rate of adsorption, and β (g/mg) is related to the activation energy and extent of surface coverage for chemisorption during the adsorption experiment.

2.6. Determination of Pb^{2+} concentration

The concentration of Pb^{2+} was determined according to the American Public Health Association (APHA) method [20] using atomic absorption spectrophotometer (Varian Spectra AA 220, USA) with graphite furnace and equipped with deuterium arc background corrector. The precision of the metal measurement was determined by analyzing samples in triplicate, and for each series of measurements, an absorption calibration curve was constructed.

3. Results and discussion

3.1. Characterization of the prepared materials

The preparation and characterization of the newly prepared material, IHPC, were extensively discussed in our previous paper [14]. Briefly, the prepared material has large mesopore volume in addition to the macroporosity. The Fourier transform infrared (FTIR) analysis revealed the presence of carboxyl, carbonyl, alcoholic and phenolic hydroxyl group and C=C stretching as a surface functional groups on the prepared materials [14].

In order to get a clear picture about the contribution of surface function groups in the adsorption of Pb^{2+}, FTIR analysis (Fig. 1) was carried out for the studied adsorbents (IHPC, IHA and PC) before and after the adsorption of lead.

Fig. 1 shows that the major infrared bands in the three adsorbents are at around 3,420; 2,920; 1,720; 1,610; 1,410; 1,250; 1,170; and 1,033 cm^{-1}, which correlated to phenolic hydroxyl stretching; aliphatic C–H stretching; carboxyl and carbonyl C=O stretching; aromatic C=C stretching; C–H bending of the CH_2 and CH_3 groups; C–O stretching and O–H deformation of COOH; alcoholic hydroxyl stretching; and C–O stretching of polysaccharide substances, respectively [14]. In Fig. 1(c) (IHPC samples), it could be observed that, the band at 1,167 cm^{-1} corresponding to alcoholic hydroxyl stretching disappeared after the adsorption of Pb^{2+}. Moreover, it could be observed that there is a considerable shift in the bands 3,432; 1,610; 1,410 and 1,033 after the adsorption of Pb^{2+} indicating that the adsorption takes place on these surface functional groups. Therefore, the adsorption process might be chemisorption process.

3.2. Adsorption study

3.2.1. Contact time effect

Fig. 2 represents the effect of contact time on adsorption of Pb^{2+} ions using PC, IHA and IHPC. The results revealed that the adsorption of Pb^{2+} takes place in two steps: the first step (the first 10 min), the rate of adsorption is very rapid, then the rate slows down, and the adsorption increased gradually till the equilibrium was attained at 25 min for PC, and 30 min for both IHA and IHPC. Therefore, the optimum contact time for the adsorption of Pb^{2+} was set at 25 min for PC and 30 min for IHA and IHPC. It is clearly observed from Fig. 3 that (a) IHPC and IHA remove 99.82% and 96.47%, respectively, after 30 min, while for PC, the maximum adsorption (92.35%) was attained at 25 min, and (b) IHPC has the highest adsorption capacity for Pb^{2+} among the adsorbents used in this study. Therefore, mounting of humic acid on PC introduced a new material having higher affinity for lead ions than pure PC and IHA.

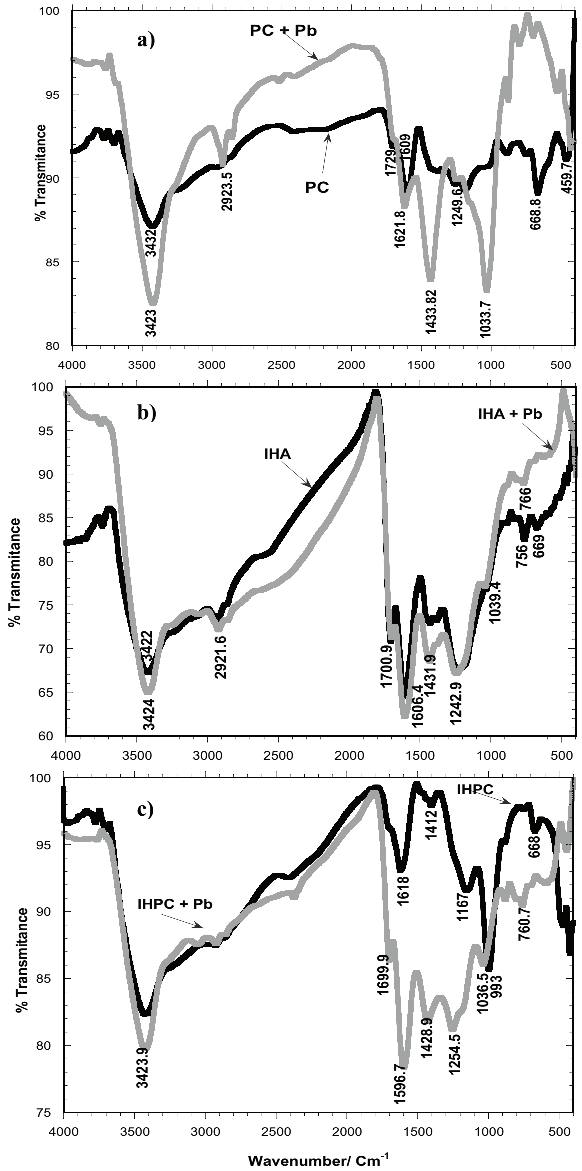

Fig. 1. FTIR of: (a) PC, (b) IHA and (c) IHPC before and after the adsorption of Pb^{2+}.

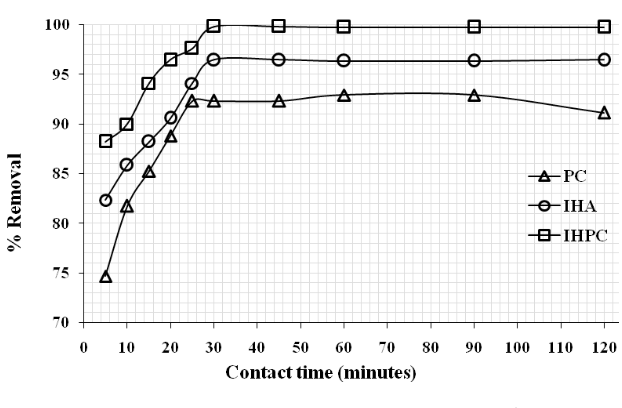

Fig. 2. Effect of contact time on the adsorption of Pb^{2+} onto IHA, IHPC and PC (adsorbent dose, 0.5 g/L; initial concentration, 20 mg/L; pH, 5.3).

3.2.2. pH effect

pH was identified as the main parameter that controls the process of metal sorption [21]. This is attributed to (a) the strong competition between proton and Pb^{2+} in acid medium, (b) the pH effect on the chemical precipitation of Pb^{2+} at higher pH values and (c) ionization of surface functional groups on the adsorbents. Therefore, selection of pH is a significant point for the adsorption of Pb^{2+} by the adsorbents in the current study [22,23]. The pH effect on the adsorption of Pb^{2+} ions is given in Fig. 3. The results indicated that the adsorption of Pb^{2+} increased with increasing pH values. This might be caused by the formation of hydronium ions at low value of pH, which limits the approach of Pb^{2+} to the adsorbent surface through repulsive forces. Also, hydronium ions might compete with Pb^{2+} to occupy the adsorption sites. Moreover, at high pH the IHA surface starts to have a negative charge, which makes an electrostatically favorable situation for higher Pb^{2+} adsorption.

The maximal percentage removal of Pb^{2+} was 99.95%, 97.75% and 95% for IHPC, IHA and PC, respectively, indicating that IHPC has higher affinity for Pb^{2+} than IHA and PC. Since a chemical precipitation of Pb^{2+} was expected to take place at pH 6.5 as reported in literature [15] so a pH of 6.2 was used as the optimum value in the rest of experiment.

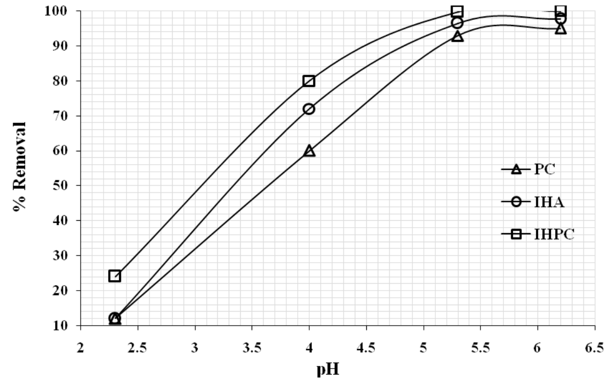

Fig. 3. Effect of pH on the adsorption of Pb^{2+} onto IHA, IHPC and PC (adsorbent dose: 0.5 g/L; initial concentration: 20 mg/L; contact time: 25 min for PC and 30 min for IHA and IHPC).

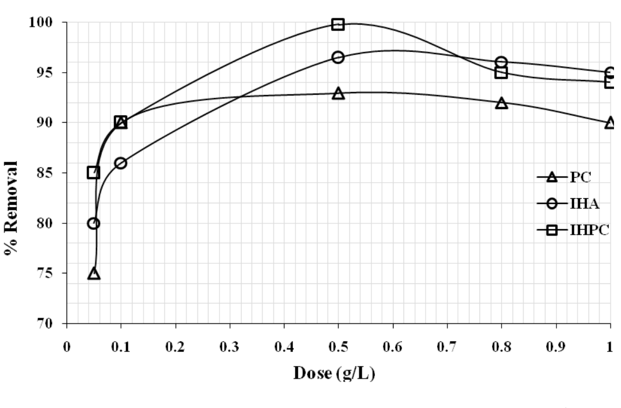

Fig. 4. Effect of adsorbent dose on the adsorption of Pb^{2+} onto IHA, IHPC and PC (initial concentration: 20 mg/L; pH: 6.2; contact time: 25 min for PC and 30 min for IHA and IHPC).

3.2.3. Effect of adsorbent dose

The effect of adsorbent dosage is illustrated in Fig. 4. The data indicated that the adsorption of Pb^{2+} was increased with the subsequent increase in the adsorbent dose and nearly became stable at dosage higher than 0.5 g/L for the three adsorbents under study. This behavior was attributed to the formation of aggregates at higher dosage of adsorbents that decreases the available surface area for adsorption. Thereafter, a dosage of 0.5 g/L was used as optimum value in the rest of study.

3.2.4. Effect of lead ion concentration on the distribution constant K_d

The distribution ratio K_d for the adsorption of Pb^{2+} onto IHPC, IHA and PC as a function of the initial concentration of Pb^{2+} ions in solution was studied at constant temperature (25°C ± 0.1°C). K_d was calculated as follows [24]:

$$\mathrm{K}_d = \left(\frac{\text{amount of metal in adsorbent}}{\text{amount of metal in solution}}\right)\frac{V}{m} \tag{9}$$

where m is the amount of adsorbent (g), and V is the used volume of solution (mL).

Fig. 5 shows K_d as a function of Pb^{2+} concentration. The data revealed that the K_d values were decreased with increasing Pb^{2+} initial concentration. This might be due to the occupation of the less energetically favored sites with increasing Pb^{2+} concentration in solution.

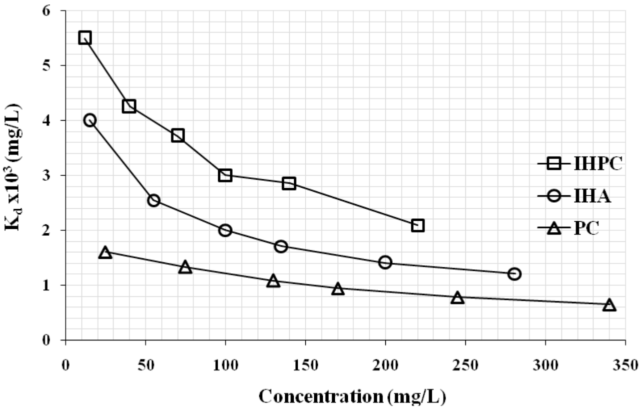

Fig. 5. Effect of Pb^{2+} concentration on the adsorption process (initial concentration: 45–350 mg/L; adsorbent dose: 0.5 g/L; pH: 6.2).

3.3. Adsorption isotherms

3.3.1. Freundlich and Langmuir adsorption isotherms

The driven parameters of Freundlich and Langmuir adsorption isotherm models are listed in Table 1. R^2 values indicated that the Langmuir isotherm model describes the adsorption of lead to PC, IHA and IHPC better than Freundlich model. Therefore, the adsorption of lead is mainly homogeneous, and a monolayer adsorption takes place on the surface of PC, IHA and IHPC. The $q_{\max}$ (Table 1) were determined to be 714.3, 454.5 and 333.3 mg/g from Langmuir isotherm for IHPC, IHA and PC, respectively. IHPC has higher adsorption capacity than IHA and PC indicating that mounting of IHA on PC was successful and beneficial in improving the adsorptive characteristics of IHA and PC. Moreover, IHPC has superior adsorption capacity for lead when compared with literature. For example, Baker and Khalili [25] reported $q_{\max}$ value of 60.241 mg/g for lead by IHA at pH 4 and temperature 65°C. Chen et al. [26] reported $q_{\max}$ value of 58 mg/g for lead by hydrogel of starch immobilized humic acid. Also, $q_{\max}$ values of 27.5 and 2.8 mg/g were reported [27,28] for lead adsorption by pine cone activated carbon and manganese oxide modified activated carbon, respectively.

To further investigate the adsorption intensity, the dimensionless constant separation factor (R_L) was calculated according to the following equation:

$$R_L = \frac{1}{1 + b\,C_e} \tag{10}$$

The R_L value gives indication on the nature of the adsorption process. It has been argued that the adsorption process is unfavorable if $R_L > 1$; linear if $R_L = 1$; favorable if $0 < R_L < 1$ and irreversible if $R_L = 0$.

The R_L values obtained for the materials under study were in the range of 0.3–0.9 for IHPC, 0.29–0.86 for IHA and 0.34–0.87 for PC. These results indicate that the adsorption process of lead ions onto the prepared materials is favorable.

3.3.2. Dubinin–Radushkevich (D–R) isotherm

The data in Table 1 illustrate the D–R driven parameter for the adsorption of Pb^{2+} onto PC, IHA and IHPC. It is well documented that the calculated mean free energy of adsorption (E) can provide a knowledge about the mechanism of adsorption, physical or chemical. If E value in the range from 8 to 16 kJ/ mol, the adsorption takes place chemically, while if

Table 1
Summary of isotherm model parameters for the adsorption of Pb^{2+} onto IHPC, IHA and PC (adsorbent dose: 0.5 g/L; initial concentration: 45–350 mg/L; pH: 6.2)

Adsorbent	Langmuir			Freundlich			Dubinin–Radushkevich (D–R)			
	K	$q_{\max}$	R^2	K_f	n	R^2	X_m	β	E	R^2
IHPC	0.008	714.3	0.984	13.02	1.47	0.986	0.0182	-6.914×10^{-9}	8.504	0.997
IHA	0.0084	454.54	0.991	12.87	1.7	0.989	0.0109	-6.866×10^{-9}	8.533	0.992
PC	0.005	333.3	0.998	4.49	1.37	0.98	0.0071	-7.12×10^{-9}	8.38	0.993

Note: K (L/mg) is the equilibrium adsorption constant; $q_{\max}$ (mg/g) is the maximum amount of metal ion adsorbed per unit mass of adsorbent; X_m (mol/g) is the maximum adsorption capacity; β (mol^2/J^2) is constant related to the activation energy and extent of surface coverage; and E (KJ/mol) is the adsorption energy.

Table 2
Pseudo-first-order and pseudo-second-order kinetic models for Pb^{2+} adsorption onto PC, IHA and IHPC (adsorbent dose: 0.5 g/L; initial concentration: 20 mg/L; pH: 6.2)

Adsorbent	$q_{e,\mathrm{exp.}}$	Pseudo-first-order model			Pseudo-second-order model		
		K_1	$q_{e,\mathrm{cal.}}$	R^2	K_2	$q_{e,\mathrm{cal.}}$	R^2
IHPC	39.94	0.096	8.68	0.9870	0.0353	40.32	0.9999
IHA	39.00	0.125	13.02	0.9199	0.0471	38.91	0.9998
PC	38.00	0.132	19.11	0.8757	0.0261	38.31	0.9997

Note: $q_{e,\mathrm{exp.}}$ (mg/g): experimental q_e values and $q_{e,\mathrm{cal}}$. (mg/g): calculated q_e values.

energy value is less than 8 kJ/mol, the adsorption occurs physically [29]. In the current study, the mean adsorption energy (Table 1) was 8.504, 8.533 and 8.38 kJ/mol for the adsorption of Pb^{2+} onto IHPC, IHA and PC, respectively, indicating that the adsorption of Pb^{2+} takes place chemically on the surface functional groups.

3.4. Adsorption kinetics

3.4.1. Pseudo-first-order model

Table 2 shows the obtained data for the first-order model. This model failed to introduce a real estimation of the q_e of adsorbed Pb^{2+} onto IHPC, IHA and PC since the experimental values of q_e were much higher than the fitted values in spite of the correlation coefficient R^2 are comparatively high. This indicated that the first-order reaction cannot describe the adsorption of Pb^{2+} onto IHPC, IHA and PC.

3.4.2. Pseudo-second-order model

The plot of t/q_t vs. t according to Eq. (7) gave straight lines for the adsorption of Pb^{2+} onto IHPC, IHA and PC. The rate constant of the second-order k_2 and q_e were calculated from the slope and the intercept (Table 2). The obtained values of q_e from this model were very close to experimental values, a first indicator for the suitability of this model. The R^2 values obtained from this model were 0.9999, 0.9998 and 0.9997 for the adsorption of Pb^{2+} onto IHPC, IHA and PC, respectively.

3.4.3. Elovich model

The correlation coefficients R^2 obtained by Elovich model were 0.708, 0.7393 and 0.7993 for PC, IHA and IHPC, respectively. This revealed that the Elovich model was not appropriate for fitting the adsorption data of lead ions onto the prepared adsorbent materials used in the current study.

3.4.4. Intraparticle diffusion model

In order to explore the adsorption mechanism, the obtained data were tested by the intraparticle diffusion model. The sorption might be described through three successive steps: (i) adsorption across the external boundary layer film, (ii) adsorption at the site on adsorbent surface (this step is often proposed to be very rapid) and (iii) the diffuse of adsorbate molecules by a pore diffusion processor through solid surface diffusion mechanism [30].

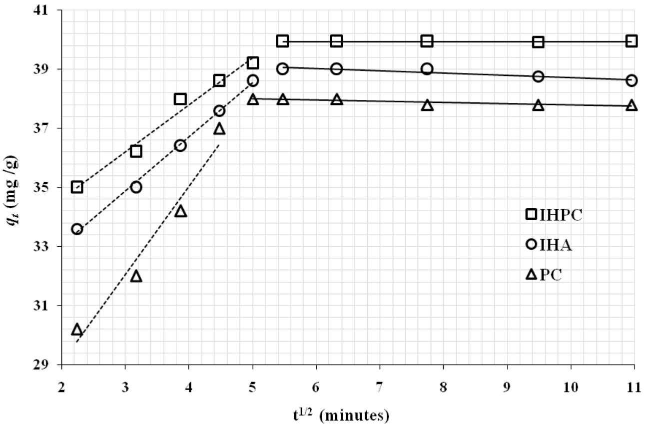

Fig. 6. Intraparticle diffusion kinetics of Pb^{2+} adsorption onto IHPC, IHA and PC (adsorbent dose: 0.5 g/L; initial concentration: 20 mg/L; pH: 6.2).

The Weber's diffusion model can describe the intraparticle diffusion model as follows [31]:

$$q_t = k_p t^{1/2} + C \tag{11}$$

where k_p is the rate constant of the intraparticle diffusion (mg/g $\mathrm{min}^{1/2}$) and the rate constant for the intraparticle transport C expressed in mg/g $\mathrm{min}^{1/2}$.

If the plot of q_t vs. $t^{1/2}$ gave a straight line passing through the origin, then the adsorption of the ions follows a diffusion mechanism. While, when pore diffusion describe the adsorption process, the relationship will be non-linear.

Fig. 6 indicated that the lines do not pass through the origin and the adsorption process comprises two phases: the initial portion reveals external mass transfer while the linear portion is due to pore intraparticle or film diffusion. This suggests that the intraparticle diffusion is not the rate-limiting step for the adsorption and both intraparticle diffusion and film diffusion might be the rate-limiting steps for the adsorption of Pb^{2+} onto the prepared adsorbents.

To test whether the adsorption takes place through intraparticle diffusion or film diffusion mechanism, the results have been analyzed by the Boyd's kinetic model [32]. The simple form of the rate equation can be represented by:

$$F = 1 - \frac{6}{\pi^2} \sum_{m=1}^{\infty} \frac{1}{m^2} \exp\left[-m^2 Bt\right] \tag{12}$$

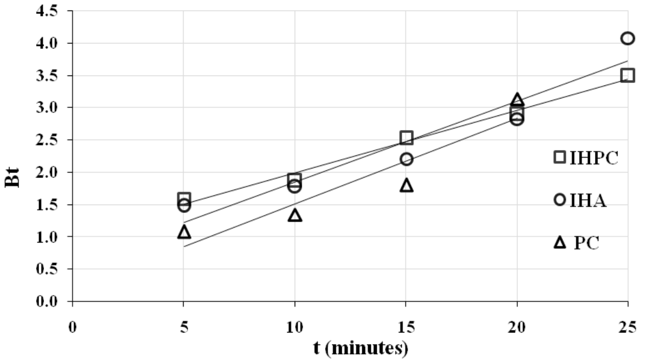

Fig. 7. Boyd plot of Pb^{2+} adsorption onto IHPC, IHA and PC (adsorbent dose: 0.5 g/L; initial concentration: 20 mg/L; pH: 6.2).

where F (q_e/q_t) is the fractional attainment of equilibrium at time t and the time constant B (min^{-1}) calculated by Eq. (13):

$$B = \frac{D_i \pi^2}{r^2} \tag{13}$$

D_i is the effective diffusion coefficient of the adsorbate in the sorbent phase (cm^2/min); r is the radius of the adsorbent particle (cm); and m is an integer that defines the infinite series solution. B_t is given by Eq. (14):

$$B_t = -0.4977 - \ln(1-F) \tag{14}$$

If the plot of B_t vs. t gave a straight line passes through the origin, this indicating that the adsorption process is controlled by the particle-diffusion mechanisms. Otherwise, the adsorption is controlled by the film diffusion. From Fig. 7, it is clear that the plots are neither linear nor passes through the origin which reveals that the intraparticle diffusion is the rate-controlling step with the film diffusion.

4. Conclusion

From the current study, it could be concluded that the IHPC as an inexpensive new material exhibited much higher affinity for adsorption of Pb^{2+} than PC and IHA. The kinetics of the adsorption studies revealed that the adsorption of Pb^{2+} obeys the second-order model. Langmuir adsorption isotherm was found to be the best isotherm model to describe the adsorption of lead ions onto the three adsorbents with $R^2 > 0.98$. The maximum adsorption capacity order was IHPC > IHA > PC. The IHPC as a prepared new material can be used as an efficient adsorbent for practical application in water and wastewater treatment.

References

[1] A. Kunz, P. Peralta-Zamora, S.G. de Moraes, N. Durán, New trends in the treatment of textile effluents, New chemistry, 25 (2002) 78–82.

[2] D. Mohan, H. Kumar, A. Sarswat, M. Alexandre-Franco, C.U. Pittman, Cadmium and lead remediation using magnetic oak wood and oak bark fast pyrolysis bio-chars, Chem. Eng. J., 236 (2014) 513–528.

[3] X. Zhang, S. Lin, X.-Q. Lu, Z.-l. Chen, Removal of Pb(II) from water using synthesized kaolin supported nanoscale zero-valent iron, Chem. Eng. J., 163 (2010) 243–248.

[4] WHO, Guidelines for Drinking-water Quality, World Health Organization, Geneva, p. 973, 2008.

[5] W. Lo, H. Chua, K.-H. Lam, S.-P. Bi, A comparative investigation on the biosorption of lead by filamentous fungal biomass, Chemosphere, 39 (1999) 2723–2736.

[6] M. Lasheen, I.Y. El-Sherif, D.Y. Sabry, S. El-Wakeel, M. El-Shahat, Removal of heavy metals from aqueous solution by multiwalled carbon nanotubes: equilibrium, isotherms, and kinetics, Desal. Wat. Treat., 53 (2015) 3521–3530.

[7] Y.-H. Li, Z. Di, J. Ding, D. Wu, Z. Luan, Y. Zhu, Adsorption thermodynamic, kinetic and desorption studies of Pb^{2+} on carbon nanotubes, Water Res., 39 (2005) 605–609.

[8] A.A. El-Kady, R. Carleer, J. Yperman, J. D'Haen, H.H. Abdel Ghafar, Kinetic and adsorption study of Pb(II) toward different treated activated carbons derived from olive cake wastes, Desal. Wat. Treat., 57 (2016) 8561–8574.

[9] W.W. Ngah, M.A.K.M. Hanafiah, Removal of heavy metal ions from wastewater by chemically modified plant wastes as adsorbents: a review, Bioresour. Technol., 99 (2008) 3935–3948.

[10] L. Largitte, T. Brudey, T. Tant, P.C. Dumesnil, P. Lodewyckx, Comparison of the adsorption of lead by activated carbons from three lignocellulosic precursors, Microporous Mesoporous Mater., 219 (2016) 265–275.

[11] R. Mailler, J. Gasperi, Y. Coquet, C. Derome, A. Buleté, E. Vulliet, A. Bressy, G. Varrault, G. Chebbo, V. Rocher, Removal of emerging micropollutants from wastewater by activated carbon adsorption: experimental study of different activated carbons and factors influencing the adsorption of micropollutants in wastewater, J. Environ. Chem. Eng., 4 (2016) 1102–1109.

[12] Q. Jiuhui, Research progress of novel adsorption processes in water purification: a review, J. Environ. Sci., 20 (2008) 1–13.

[13] O. Gezici, H. Kara, S. Yanık, H.F. Ayyildiz, S. Kucukkolbasi, Investigating sorption characteristics of copper ions onto insolubilized humic acid by using a continuously monitored solid phase extraction technique, Colloids Surf., A, 298 (2007) 129–138.

[14] E.K. Radwan, H.H.A. Ghafar, A.S. Moursy, C.H. Langford, A.H. Bedair, G. Achari, Preparation and characterization of humic acid–carbon hybrid materials as adsorbents for organic micro-pollutants, Environ. Sci. Pollut. Res., 22 (2015) 12035–12049.

[15] N.N. Nassar, Rapid removal and recovery of Pb(II) from wastewater by magnetic nanoadsorbents, J. Hazard. Mater., 184 (2010) 538–546.

[16] H.K. Boparai, M. Joseph, D.M. O'Carroll, Kinetics and thermodynamics of cadmium ion removal by adsorption onto nano zerovalent iron particles, J. Hazard. Mater., 186 (2011) 458–465.

[17] S. Lagergren, About the theory of so-called adsorption of soluble substances, K. Sven. Ventansk.akad. Handl., 24 (1898) 1–39.

[18] Y.S. Ho, G. McKay, D.A.J. Wase, C.F. Forster, Study of the sorption of divalent metal ions on to peat, Adsorpt. Sci. Technol., 18 (2000) 639–650.

[19] S. Chien, W. Clayton, Application of Elovich equation to the kinetics of phosphate release and sorption in soils, Soil Sci. Soc. Am. J., 44 (1980) 265–268.

[20] APHA, Standard Methods for the Examination of Water and Wastewater, 21st ed., APHA, AWWA, WEF, Washington, D.C., USA, 2005.

[21] D. Kratochvil, B. Volesky, Advances in the biosorption of heavy metals, Trends Biotechnol., 16 (1998) 291–300.

[22] P. King, N. Rakesh, S. Beenalahari, Y.P. Kumar, V. Prasad, Removal of lead from aqueous solution using *Syzygium cumini* L.: equilibrium and kinetic studies, J. Hazard. Mater., 142 (2007) 340–347.

[23] S. Yao, J. Zhang, D. Shen, R. Xiao, S. Gu, M. Zhao, J. Liang, Removal of Pb(II) from water by the activated carbon modified by nitric acid under microwave heating, J. Colloid Interface Sci., 463 (2016) 118–127.

[24] T.K. Naiya, A.K. Bhattacharya, S.K. Das, Adsorption of Cd(II) and Pb(II) from aqueous solutions on activated alumina, J. Colloid Interface Sci., 333 (2009) 14–26.

[25] H. Baker, F. Khalili, Analysis of the removal of lead(II) from aqueous solutions by adsorption onto insolubilized humic acid: temperature and pH dependence, Anal. Chim. Acta, 516 (2004) 179–186.

[26] R. Chen, Y. Zhang, L. Shen, X. Wang, J. Chen, A. Ma, W. Jiang, Lead(II) and methylene blue removal using a fully biodegradable hydrogel based on starch immobilized humic acid, Chem. Eng. J., 268 (2015) 348–355.

[27] M. Momčilović, M. Purenović, A. Bojić, A. Zarubica, M. Ranđelović, Removal of lead(II) ions from aqueous solutions by adsorption onto pine cone activated carbon, Desalination, 276 (2011) 53–59.

[28] S.M. Lee, D. Tiwari, Manganese oxide immobilized activated carbons in the remediation of aqueous wastes contaminated with copper(II) and lead(II), Chem. Eng. J., 225 (2013) 128–137.

[29] A. Sarı, M. Tuzen, Biosorption of Pb(II) and Cd(II) from aqueous solution using green alga (*Ulva lactuca*) biomass, J. Hazard. Mater., 152 (2008) 302–308.

[30] W. Cheung, Y. Szeto, G. McKay, Intraparticle diffusion processes during acid dye adsorption onto chitosan, Bioresour. Technol., 98 (2007) 2897–2904.

[31] W.J. Weber, J.C. Morris, Kinetics of adsorption on carbon from solution, J. Sanit. Eng. Div., 89 (1963) 31–60.

[32] G. Boyd, A. Adamson, L. Myers Jr., The exchange adsorption of ions from aqueous solutions by organic zeolites. II. Kinetics[1], J. Am. Chem. Soc., 69 (1947) 2836–2848.